

Experimental control of coherence of a chaotic oscillatorS. Boccaletti,¹ E. Allaria,² and R. Meucci¹¹*Istituto Nazionale di Ottica Applicata, Largo Enrico Fermi, 6 I50125 Florence, Italy*²*Department of Physics, University of Florence, Florence, Italy*

(Received 24 October 2003; revised manuscript received 24 February 2004; published 15 June 2004)

We give experimental evidence that a delayed feedback control strategy is able to efficiently enhance the coherence of an experimental self-sustained chaotic oscillator obtained from a CO₂ laser with electro-optical feedback. We demonstrate that coherence control is achieved for various choices of the delay time in the feedback control, including values that would lead to the stabilization of an unstable periodic orbit embedded within the chaotic attractor. The relationship between the two processes is discussed.

DOI: 10.1103/PhysRevE.69.066211

PACS number(s): 05.45.Xt, 05.45.Gg

A very relevant feature that characterizes self-sustained oscillators is the coherence, or constancy of their oscillation frequency. Its control is a fundamental task in various practical applications, e.g., at the moment of improving the reliability of electronic and optical sources, as well as for enhancing the quality of mechanical clocks. For coupled or forced chaotic oscillators it represents a crucial parameter determining their capability to give rise to a phase synchronized motion [1–3].

Phase synchronization (PS) refers to a process related to the presence of two distinct self-sustained oscillators whose original different rhythms are adjusted by means of a weak coupling, even when the corresponding amplitudes are only feebly correlated. In the chaotic case, it has been shown that PS occurs only for some phase coherent oscillators [1,2], while systems having a rather broad distribution of time scales in their unstable periodic orbits only display imperfect PS [4].

By calling $\phi(t)$ the phase of an oscillator, phase coherence can be quantified by means of the so-called phase diffusion coefficient

$$D_\phi \propto \lim_{t \rightarrow \infty} \frac{1}{t} \langle [\phi(t) - \langle \phi(t) \rangle]^2 \rangle, \quad (1)$$

where $\langle \dots \rangle$ stays for a time average. While the above definition rigorously holds only for periodic oscillators subjected to noisy Gaussian fluctuations, it has been recently proposed that such a measure could also be applied for chaotic oscillators, under the assumption that the deterministic chaotic fluctuations of the phase could be considered as noisy Gaussian contributions [3,5]. In particular, it has been numerically shown that a delayed feedback control strategy [6] may modify the value of D_ϕ for nonphase coherent chaotic oscillators, leading in some cases to an enhancement of the coherence of the motion [5], inducing a drastic reduction of D_ϕ and allowing such otherwise nonphase synchronizable oscillators to eventually phase synchronize with external forcings. The fact that control of coherence can improve phase synchronizability is a relevant property, since PS of chaotic systems is a rather ubiquitous phenomenon in nature [7], in controlled laboratory experiments [8], and in space extended or infinite dimensional systems [9].

In this paper we give, to our knowledge, the first experimental evidence of control of coherence in a self-sustained chaotic oscillator, and we discuss how this process is related to the stabilization of unstable periodic orbits (UPOs) embedded within a chaotic attractor [10].

The experimental setup is shown in Fig. 1(a). It consists of a single mode CO₂ laser with electro-optic feedback. Precisely, a slow flow gas mixture of CO₂ at a pressure of 28 mbar, pumped by a dc discharge current of 6 mA (the pump threshold for the lasing action being 3 mA), is inserted within the laser cavity defined by a partially (M_2) and a totally (M_1) reflecting mirror. The cavity houses also an antireflection coated CdTe electro-optic modulator (EOM) for amplitude modulations. The laser output intensity is detected by a fast HgCdTe diode detector D whose electric output is sent into a feedback loop, including an amplifier R and a bias voltage B_0 . The output of the amplifier is taken to drive the EOM component. It is known that depending on the two control parameters of the feedback loop (the gain R and the bias voltage B_0 on the amplifier), different chaotic regimes can be observed for the behavior of the laser output intensity [11,12]. In this work we set the control parameters in conditions where the laser intensity is locally confined around an unstable fixed point ($R=9$ and $B_0=400$ mV). In these conditions a chaotic regime is reached after a sequence of subharmonic bifurcations on a limited cycle originated from a Hopf bifurcation [13]. The resulting temporal evolution of the laser intensity I can be seen in Fig. 1(b). Furthermore, a time delayed embedding reconstruction of the corresponding attractor (with embedding time $\tau=6$ μ s) is shown in Fig. 1(c). In these experimental conditions, the dynamics can be conveniently represented by a six-variable model system [14]. For the parameters used in our experiment, such a model gives a maximum Lyapunov exponent Λ of about 11 900 s⁻¹. The corresponding Lyapunov time ($1/\Lambda$) amounts to about 1.2 times the length of the period 1 UPO ($T_1 \approx 70$ μ s).

In order to control the coherence of the chaotic oscillator, we use a second feedback loop, consisting of a digital delay line with 12 bit amplitude resolution and a delay time T_d that can be set with 0.5 μ s of resolution. The difference between the laser output intensity signal $I(t)$ and its delayed version $I(t-T_d)$ is amplified with a gain G and used as an additive signal in the main feedback loop [see Fig. 1(a)]. This scheme

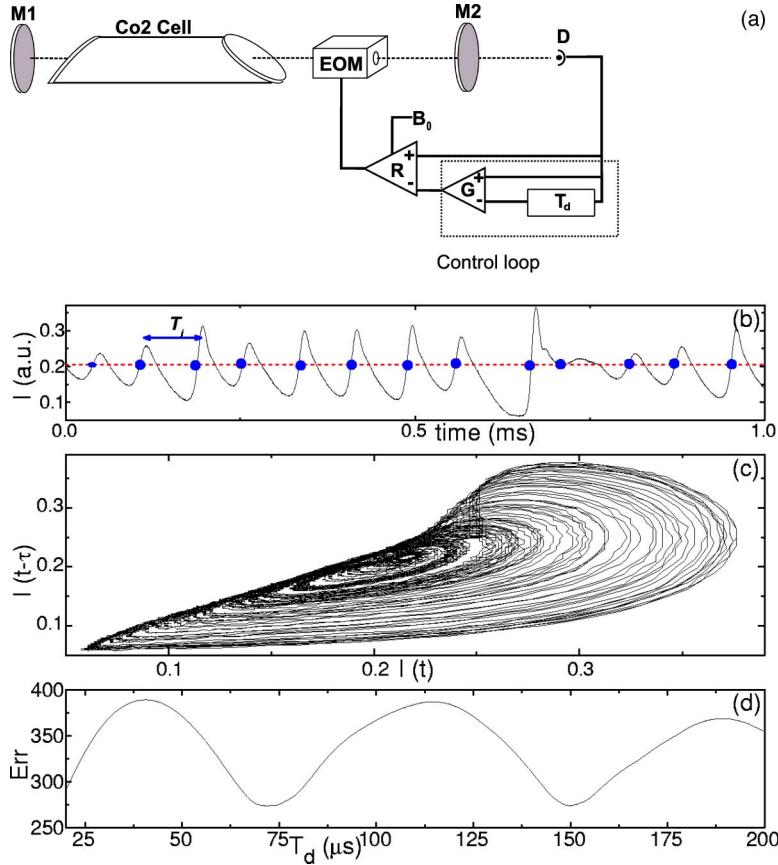


FIG. 1. (a) Experimental setup. M_1 and M_2 , mirrors; EOM, electro-optical modulator; D , diode detector; T_d , delay; G and R , amplifiers; and B_0 , applied bias voltage. (b) Snapshot of the time sequence of the output intensity I (in arbitrary units) for the uncontrolled case. The dashed line represents the level taken for determining passages onto the Poincaré section (with the additional condition of the signal having a positive temporal derivative). Points depict the sequence of passage times onto the Poincaré section. The arrow marked with the label τ_i illustrates the way in which the sequence of time intervals between two successive crossings of the Poincaré section has been obtained. (c) Time-delayed embedding reconstruction of the attractor corresponding to the uncontrolled case. Both axes are in arbitrary units. The embedding time is $\tau=6 \mu\text{s}$. (d) Error function $\text{Err}(T_d)$ (in arbitrary units, see text for definition) vs T_d (in micro second) calculated from a long data series of the output intensity with no feedback ($G=0$).

is an experimental implementation of the so-called *time-delayed autosynchronization* (TDAS) method proposed by Pyragas [6], which is able to stabilize UPOs embedded within the chaotic attractor, for suitable choices of T_d and G . The reliability of TDAS for UPOs stabilization in lasers was experimentally proven in both the externally driven [15] and the autonomous [14] cases.

The unperturbed chaotic dynamics embeds an infinite number of UPOs. In Fig. 1(d) we report the error function $\text{Err}(T_d) = (1/N) \sum_{i=1, \dots, N} |I(t_i) - I(t_i - T_d)|$ for an $N=5000$ data series of the output time intensity $I(t)$ with no feedback ($G=0$) and sampled with a time interval $t_i - t_{i-1} = 0.4 \mu\text{s}$. The local minima of $\text{Err}(T_d)$ mark the values of T_d that correspond to UPO's periods. In particular, Fig. 1(d) shows that the length of the period 1 (the period 2) UPOs is approximately equal to $T_d=70 \mu\text{s}$ ($T_d=140 \mu\text{s}$). In the following we will set the delay time T_d of the control loop at 70, 100, and 140 μs , and vary the gain G for the three cases. In particular, fixing $T_d=70 \mu\text{s}$ ($T_d=140 \mu\text{s}$), i.e., matching the period T_1 (the period T_2), and increasing G would eventually lead to the stabilization of period 1 (of period 2) UPO, while for $T_d=100$, we are in working conditions in which no UPOs can be stabilized [as it can be seen from Fig. 1(d)].

In all measurements, we introduce a suitable threshold $\Theta=0.205$. When the output intensity crosses Θ for the n th time with a positive temporal derivative, we associate such an event to the n th crossing of the chaotic trajectory on the Poincaré section of the attractor, and record the corresponding value of the time t_n . As illustrated in Fig. 1(b), this strategy allows us to easily calculate the sequence $\{\tau_n\}$ of recur-

rent times or crossing time intervals on the Poincaré section ($\tau_n \equiv t_n - t_{n-1}$). The values of Θ has been carefully selected to assure that the signal encounters the Poincaré section once at each oscillation.

By linear interpolation between successive crossings on the Poincaré section, the sequence $\{\tau_n\}$ gives immediately a measure of the instantaneous phase $\phi(t)$ of the chaotic oscillator [3],

$$\phi(t) = 2\pi k + 2\pi \frac{t - \tau_k}{\tau_{k+1} - \tau_k} \quad (\tau_k < t < \tau_{k+1}), \quad (2)$$

where the integer k marks the k th crossing of the trajectory on the Poincaré section.

By recording long sequences of recurrent times (about 10 000 for each measurement), we are able to calculate the phase diffusion coefficient (1), as well as the coherence factor [16]

$$C = \frac{\langle \tau \rangle}{[\sigma_{\{\tau_n\}}]^{1/2}}, \quad (3)$$

where $\langle \tau \rangle$ ($\sigma_{\{\tau_n\}}$) denotes the average value (the standard deviation) of the distribution of the recurrent times $\{\tau_n\}$.

We start by setting $T_d=100 \mu\text{s}$ and gradually increasing G . In this condition, T_d is far from matching the length of the period 1 UPO, and therefore no values of G can stabilize a UPO. Figure 2(a) reports the coherence factor C [Eq. (3)] in logarithmic scale vs the gain G in the control loop. As it can be seen the coherence factor increases monotonically, as the

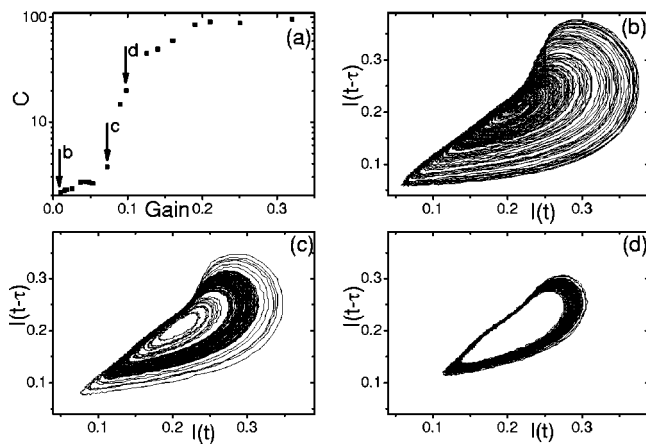


FIG. 2. (a) Coherence factor C (see text for definition) in logarithmic scale vs gain G in the control loop for $T_d=100 \mu s$. The three arrows indicate the values of G at which (b)–(d) were obtained. (b)–(d) Time-delayed embedding reconstruction of the attractor (embedding time $\tau=6 \mu s$) for $G=0.01$ (b), $G=0.07$ (c), and $G=0.1$ (d).

gain factor increases. Figure 2 shows time delayed embedding reconstructions of the attractor for $G=0.01$ (b), $G=0.07$ (c), and $G=0.1$ (d). Looking at Fig. 2(c), one easily realizes that the control loop forces the appearance of a still chaotic motion, but with a higher coherence with respect to the unperturbed dynamics. Furthermore, by comparing Fig. 2(c) with Fig. 2(b), it can be seen that the main topological features of the chaotic attractor are only weakly changed, despite an improvement of a factor 5 in the coherence factor. A further increase in the gain factor produces a highly coherent motion that is developing very close to a limit cycle [Fig. 2(d)], thus destroying the main topological features of the original attractor.

A more quantitative analysis of the situation can be extracted by looking at Fig. 4(b), where the phase diffusion coefficient D_ϕ [Eq. (1)] is reported vs the gain G . In this figure, one can see that increasing G from 0.01 to 0.1 results

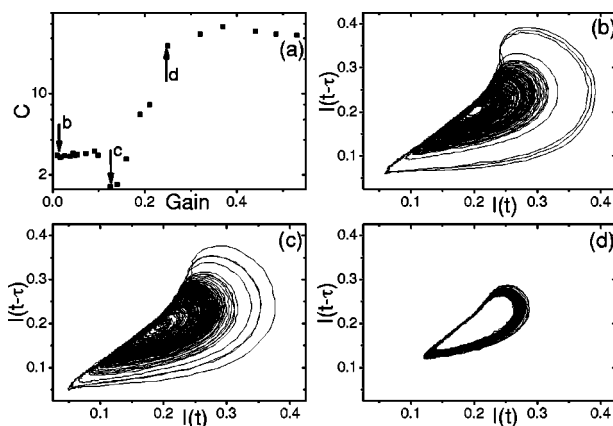


FIG. 3. (a) Coherence factor C (see text for definition) in logarithmic scale vs gain G in the control loop for $T_d=70 \mu s$. The three arrows indicate the values of G at which (b)–(d) were obtained. (b)–(d) Time-delayed embedding reconstruction of the attractor (embedding time $\tau=6 \mu s$) for $G=0.01$ (b), $G=0.12$ (c), and $G=0.25$ (d).

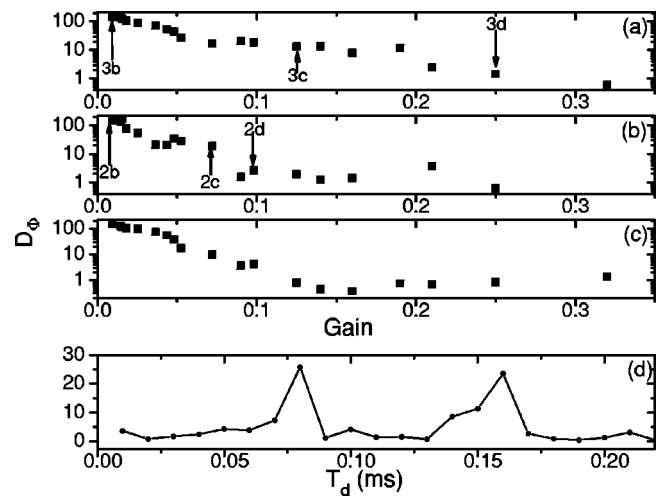


FIG. 4. (a)–(c) Phase diffusion coefficient D_ϕ (see text for definition) vs gain G in the control loop. (a) $T_d=70 \mu s$; (b) $T_d=100 \mu s$; (c) $T_d=140 \mu s$. The arrows in (a) and (b) refer to the values of G at which Figs. 2(b)–2(d) and 3(b)–3(d) were obtained. (d) Phase diffusion coefficient D_ϕ vs the delay time T_d at fixed $G=0.98$ in the feedback loop.

in a giant improvement of the coherence of the motion, in which D_ϕ is reduced by almost two orders of magnitude.

A different scenario emerges when setting $T_d=70 \mu s$ in the control loop. Now, T_d matches exactly the length of the period 1 UPO, and therefore the control loop eventually leads to the stabilization of such a UPO for $G>0.3$. As a result, coherence control here can be seen as a preliminary control step in the transition toward the stabilization of the period 1 UPO. The coherence factor C in logarithmic scale vs G is reported in Fig. 3(a). Initially ($G \leq 0.1$) there is no apparent improvement in the coherence of the recurrent times sequence. A typical attractor in this regime is shown in Fig. 3(b). Around $G=0.12$ the system sets in a chaotic state corresponding to an even less coherence in the recurrent times sequence. The corresponding chaotic attractor is shown in Fig. 3(c). Finally, for $G>0.12$ we enter the stabilization process of the period 1 UPO, in which the coherence factor increases monotonically. Figure 3(d) shows the time-delayed embedding reconstruction of the attractor just before the control of the period 1 UPO.

The phase diffusion coefficient behavior is reported in Fig. 4(a), where one observes a drastic reduction in D_ϕ in the range $0 \leq G \leq 0.08$. Later, D_ϕ seems to be quite insensitive on G up to $G \sim 0.2$, when the process of stabilization of the UPO begins and D_ϕ falls down to zero.

Let us now discuss on the relationship between the control of coherence and the stabilization of a specific UPO embedded within the chaotic attractor. While the latter process (usually called *control of chaos*) is strongly limited to a very small subset of delay times T_d (those ones matching exactly the lengths of the target periodic orbits [6,10]), the former process is more general and robust, since it is effective also for values of T_d that are by far different from the UPO's periods [as it has been demonstrated in the example of Figs. 2 and 4(b)].

When T_d matches the period of some UPOs, our results indicate that control of coherence anticipates the stabilization

of the target periodic orbit. This can be understood by considering that stabilization of a UPO implies that the trajectory must repeat on the Poincaré section over an ordered finite sequence of points at an ordered sequence of times. This process can be realized only by a first regularization of the sequence of recurrent times on the Poincaré section (control of coherence) occurring at weaker control strengths and not necessarily implying a regularization the corresponding distribution of crossing points, followed by a stabilization of amplitudes that occurs at higher control forces and has the result of reducing the collection of crossing points into the finite sequence of points corresponding to the desired UPO. Such a scenario is very much similar to what happens when two slightly different chaotic systems are coupled. In this case, one first obtains a PS state at weak coupling strengths, where only phases of the subsystems are locked, while amplitudes are almost uncorrelated, followed by a complete or identical synchronization state [17] at higher coupling strengths where amplitudes lock and the chaotic trajectories of the subsystems evolve in step with each other (this latter state corresponding to the passage of a previously positive Lyapunov exponent to a negative value as a function of the coupling parameter [1,3]).

In our case, the control method first gives rise to a TDPAS (at weaker values of the gain parameter), where only coherence is controlled and the motion remains chaotic (the originally positive Lyapunov exponent remains positive), and eventually leads to a TDAS (as it was originally named in Ref. [6]) at higher values of the gain parameters, when the UPO is stabilized, and the motion is no longer chaotic (hence the originally positive Lyapunov exponent takes a negative value).

This global scenario is confirmed also in the case of $T_d = 140 \mu\text{s}$ in the control loop. In this case, T_d equals approximately the length of the period 2 UPO, and the whole process leads eventually to the stabilization of the period 2 UPO. Analogously to what happens for the case $T_d = 70 \mu\text{s}$, D_ϕ experiences here a drastic reduction as the gain G is

increased and falls down to zero in correspondence with the stabilization of the period 2 UPO [see Fig. 4(c)] that occurs for $G > 0.1$.

Finally, in Fig. 4(d) we report D_ϕ vs T_d at a fixed value of $G = 0.98$ in the feedback loop. As originally predicted in Ref. [5], Fig. 4(d) shows that under coherence control the phase diffusion cannot only be suppressed but also enhanced for other specific choices of the feedback parameters. In particular, Fig. 4(d) shows that D_ϕ is enhanced for values of T_d close to the lengths of the UPOs, meaning that setting T_d close to the period of some UPOs, the phase diffusion coefficient D_ϕ is larger than the one corresponding to T_d values not matching periods of UPOs, at least for low values of G . Even though enhancing phase diffusion of a chaotic oscillator is not that relevant for practical purposes, the evidence of such a phenomenon further supports our claims for a coherence control induced by the feedback.

In conclusion, we have reported, to our knowledge, the first experimental evidence of control of coherence in a chaotic self-sustained oscillator, a CO₂ laser system with electro-optical modulator, where a limit cycle originated from a Hopf bifurcation reaches a chaotic condition after a sequence of subharmonic bifurcations. We demonstrated that coherence control is achieved by means of application of a delayed feedback control for various choices of the delay time in the feedback control, including values that lead to the stabilization of period 1 and period 2 UPOs embedded within the chaotic attractor. In this latter case, the relationship between control of coherence and stabilization of UPOs has been discussed.

The authors thank F. T. Arecchi, A. Pikovsky, and K. Pyragas for many helpful discussions on the subject, and P. Poggi for the help in the realization of the digital delay line within the control loop. This work was partly supported by EU Contract No. HPRN-CT-2000-00158 (COSYC of SENS), and MIUR-FIRB Contract No. RBNE01CW3M_001. E.A. acknowledges support from MIUR-FIRB Contract No. RBAU01B49F_002.

-
- [1] M. G. Rosenblum, A. S. Pikovsky, and J. Kurths, *Phys. Rev. Lett.* **76**, 1804 (1996).
- [2] K. Josić and D. J. Mar, *Phys. Rev. E* **64**, 056234 (2001).
- [3] For a comprehensive review on synchronization phenomena see S. Boccaletti, J. Kurths, G. Osipov, D. Valladares, and C. Zhou, *Phys. Rep.* **366**, 1 (2002), and references therein.
- [4] M. A. Zaks, E.-H. Park, M. G. Rosenblum, and J. Kurths, *Phys. Rev. Lett.* **82**, 4228 (1999).
- [5] D. Goldobin, M. Rosenblum, and A. Pikovsky, *Phys. Rev. E* **67**, 061119 (2003).
- [6] K. Pyragas, *Phys. Lett. A* **170**, 421 (1992).
- [7] C. Schafer *et al.*, *Nature (London)* **392**, 239 (1998); P. Tass *et al.*, *Phys. Rev. Lett.* **81**, 3291 (1998); G. D. Van Wiggeren and R. Roy, *Science* **279**, 1198 (1998); A. Neiman *et al.*, *Phys. Rev. Lett.* **82**, 660 (1999); B. Blasius, A. Huppert, and L. Stone, *Nature (London)* **399**, 354 (1999).
- [8] C. M. Ticos *et al.*, *Phys. Rev. Lett.* **85**, 2929 (2000); D. Maza *et al.*, *ibid.* **85**, 5567 (2000); E. Allaria *et al.*, *ibid.* **86**, 791 (2001).
- [9] S. Boccaletti *et al.*, *Phys. Rev. Lett.* **83**, 536 (1999); H. Chaté, A. Pikovsky, and O. Rudzick, *Physica D* **131**, 17 (1999); L. Junge and U. Parlitz, *Phys. Rev. E* **62**, 438 (2000); J. Bragard, S. Boccaletti, and H. Mancini, *Phys. Rev. Lett.* **91**, 064103 (2003).
- [10] This process has been historically called *control of chaos*. For a comprehensive review on this subject see S. Boccaletti, C. Grebogi, Y.-C. Lai, H. Mancini, and D. Maza, *Phys. Rep.* **329**, 103 (2000), and references therein.
- [11] M. Ciofini, A. Labate, R. Meucci, and M. Galanti, *Phys. Rev. E* **60**, 398 (1999).
- [12] A. N. Pisarchick, R. Meucci, and F. T. Arecchi, *Phys. Rev. E* **62**, 8823 (2000).
- [13] F. T. Arecchi, W. Gadomski, and R. Meucci, *Phys. Rev. A* **34**, 1617 (1986).

- [14] R. Meucci, A. Labate, and M. Ciofini, Phys. Rev. E **56**, 2829 (1997).
- [15] S. Bielawski, D. Derozier, and P. Glorieux, Phys. Rev. E **49**, R971 (1994); D. J. Gauthier, D. W. Sukow, H. M. Concannon, and J. E. S. Socolar, *ibid.* **50**, 2343 (1994).
- [16] C. S. Zhou, J. Kurths, E. Allaria, S. Boccaletti, R. Meucci, and F. T. Arecchi, Phys. Rev. E **67**, 066220 (2003).
- [17] H. Fujisaka and T. Yamada, Prog. Theor. Phys. **69**, 32 (1983); V. S. Afraimovich, N. N. Verichev, and M. I. Rabinovich, Izv. Vyssh. Uchebn. Zaved., Radiofiz. **29**, 1050 (1986); L. M. Pecora and T. L. Carroll, Phys. Rev. Lett. **64**, 821 (1990).